Molecules and Cells

# MiR-374b Promotes Proliferation and Inhibits Apoptosis of Human GIST Cells by Inhibiting PTEN through Activation of the PI3K/Akt Pathway

Zi-Wen Long[1,2,3], Jiang-Hong Wu[2,3], Cai-Hong[2,3], Ya-Nong Wang[2,3], and Ye Zhou[2,3,*]

[1]Department of Surgery, Shigatse People's Hospital, Shigatse 857000, P.R. China, [2]Department of Gastric Cancer Surgery, Fudan University Shanghai Cancer Center, Shanghai 200032, P.R. China, [3]Department of Oncology, Shanghai Medical College, Fudan University, Shanghai 200032, P.R. China
*Correspondence: zhouyezy17@163.com
http://dx.doi.org/10.14348/molcells.2018.2211
www.molcells.org

Gastrointestinal stromal tumours (GIST) are the most common mesenchymal tumors of the gastrointestinal (GI) tract. In order to investigate a new treatment fot GIST, we hypothesized the effect of miR-374b targeting PTEN gene-mediated PI3K/Akt signal transduction pathway on proliferation and apoptosis of human gastrointestinal stromal tumor (GIST) cells. We obtained GIST tissues and adjacent normal tissues from 143 patients with GIST to measure the levels of miR-374b, PTEN, PI3K, Akt, caspase9, Bax, MMP2, MMP9, ki67, PCNA, P53 and cyclinD1. Finally, cell viability, cell cycle and apoptosis were detected. According to the KFGG analysis of DEGs, PTEN was involved in a variety of signaling pathways and miRs were associated with cancer development. The results showed that MiR-374b was highly expressed, while PTEN was downregulated in the GIST tissues. The levels of miR-374b, PI3K, AKT and PTEN were related to tumor diameter and pathological stage. Additionally, miR-374b increased the mRNA and protein levels of PI3K, Akt, MMP2, MMP9, P53 and cyclinD1, suggesting that miR-374b activates PI3K/Akt signaling pathway in GIST-T1 cells. Moreover, MiR-374b promoted cell viability, migration, invasion, and cell cycle entry, and inhibited apoptosis in GIST cells. Taken together, the results indicated that miR-374b promotes viability and inhibits apoptosis of human GIST cells by targeting PTEN gene through the PI3K/Akt signaling pathway. Thus, this study provides a new potential target for GIST treatment.

Keywords: apoptosis, gastrointestinal stromal tumor, microRNA-374b, PI3K/Akt signaling pathway, proliferation, PTEN

## INTRODUCTION

Gastrointestinal stromal tumors (GISTs) are a kind of mesenchymaltumors of thegastrointestinal (GI) tract, which have the highest presence, and the primary tumor sites of GISTs are most detected in the stomach, followed by small intestine, colon and rectum, and esophagus (Miettinen and Lasota, 2001). The malignant potential of GISTs is multiple, with about 40% of localized GISTs at initial diagnosis resulted in metastasis, and distant metastasis showed in about 10%-20% of GISTs (Lanke and Lee, 2017). In the past decade, the addition of molecular diagnosis of mutations and utilization of tyrosine kinase inhibitors (TKIs), either as neoadjuvant or adjuvant therapy with surgery or as primary therapy in non-resectable GIST, has improved patient's outcomes markedly; and additional therapeutics also are on the horizon (Valsangkar et al., 2015). Although the treatment efficacy has greatly improved, the median progression-free survival (PFS) time of patients with GISTs is only about two years (Zhu et al., 2017). Therefore, researchers are still constantly trying to find newer and better treatment options for GISTs.

Received 11 September, 2017; revised 30 January, 2018; accepted 21 March, 2018; published online 14 June, 2018

eISSN: 0219-1032

MicroRNAs (miRs) are a group of endogenous small non-coding RNA molecules, which can regulate gene expression at the post-transcriptional level (Tao et al., 2014). MiRs are associated with many cell processes such as cell development, differentiation, proliferation, carcinogenesis and apoptosis, and the dysregulation of miRs has been especially associated with various human cancers like lymphoma, colon carcinoma, gastric carcinoma, and lung carcinoma (Markou et al., 2016, Sato et al., 2017, Wang et al., 2009, Wu et al., 2010). Accumulating evidence indicates that miRs do play a role in the biological processes of GISTs, such as tumorigenesis, progression, and prognosis (Cao et al., 2016; Mogensen and Hansen, 1990; Tsang et al., 2014). A previous study showed that inhibition of miR-374b reduced cell proliferation in IgA nephropathy and PTEN can be regulated by miR-374b (Hu et al., 2015). Moreover, the expression profiling microarray data of GIST (GSE112) suggested that the expression of PTEN was significantly reduced in GIST (http://www.ncbi.nlm.nih.gov/geo). Besides, previous studies have provided evidence that miRs contribute to the activation of PI3K/Akt signaling pathway (Chen et al., 2016; Tu et al., 2016). In recent years, it has been shown that PI3K/Akt signaling pathway components are frequently altered in human cancers (Fresno Vara et al., 2004). Importantly, the PTEN, PI3K/Akt signaling pathway plays a pivotal role in cell apoptosis, growth and proliferation (Liu et al., 2017). The PTEN functions as a phosphoinositide 3-phosphatase, that antagonizes PI3K action, and cell proliferation and survival signalsarenegatively regulatedby it (Maehama, 2007). Inactivation of PTEN is a crucial event in tumorigenesis and tumor development, and in fact it has the highest frequency of mutation in cancer after the P53 gene; and currently the tumor suppressing mechanism of PTEN gene involves several pathways including the PI3K/Akt signaling pathway (Gao et al., 2009). A study of lung adenocarcinoma has verified that the PI3K/Akt signaling pathway takes an important position in the mediating of the effects of PTEN on cell proliferation, apoptosis, and cell cycle arrest in A549 cell (Lu et al., 2016). Thus, it is speculated that miR-374b may has effects on proliferation and apoptosis of human GIST cells by targeting PTEN gene through the PI3K/Akt signaling pathway and this study was expected to provide a new drug target for the treatment of human GISTs.

## MATERIALS AND METHODS

### Gene Expression Omnibus (GEO) data sets analysis

We obtained expression profiling microarray data of GIST (GSE112) and annotated probe-files from the GEO database (http://www.ncbi.nlm.nih.gov/geo), which was detected by Human Unigene I. Background correction and normalization processing of the microarray data was carried *via* Affymetrix installation package of R software (Fujita et al., 2006). Linear model - Empirical Bayes statistics from the package limma and *t* test were used to perform the nonspecific filtration of expression profiles, and then screen differentially expressed genes (DEGs) (Smyth, 2004). Enrichment analysis of signaling pathways was conducted by ClusterProfiler of R software, based on KFGG database, then to identify the main biochemical metabolic pathways and signaling pathways that DEGs involved in (Kanehisa and Goto, 2000; Yu et al., 2012).

### Ethic statement

Patients and their families offered the signed informed consent and the study was approved by Ethics Committee of Fudan University Shanghai Cancer Center and Shanghai Medical College, Fudan University.

### Study subjects

GIST tissues and adjacent normal tissues were collected from 143 patients with GIST that pathologically confirmed by surgical resection between September, 2011 and September, 2013 in Fudan University Shanghai Cancer Center and Shanghai Medical College, Fudan University, including 78 males and 65 females. The mean age of patients was 60.8 years (from 33 to 86 years). The primary tumor sites included stomach (78 cases), small intestine (44 cases), colon-rectum (8 cases) and retroperitoneum or unknown sites (13 cases). Among which, 72 cases were malignant, 19 cases borderline and 52 cases benign. The diameter of tumor was 1 to 20 cm, and the median diameter was 5 cm. All cases were identified as GIST, and all patients had received no drug therapy, radiotherapy, chemotherapy and immunotherapy before surgery. The samples were conserved in a refrigerator at -80℃.

### Hematoxylin-eosin (HE) staining

The paraffin-embedded specimens were cut into 4-μm slices and dewaxed with xylene (ZLI-9317, Zhongshan Goldenbridge Biotechnology Co., Ltd., China) twice for 5 min, and successively soaked in ethanol of 100%, 95%, 80%, and 75% and distilled water for 1 min. Then hematoxylin (C0105, Beyotime Institute of Biotechnology, China) was used to stain the slices for 5 min and rinsed with tap-water for 3 min. The slices were placed in hydrochloric acid-ethanol solution (D9891-5G, Sigma-Aldrich Co., USA) for differentiation for 30 seconds and soaked with tap-water for 15 min. Then eosin (ZLI-9612, Zhongshan Goldenbridge Biotechnology Co., Ltd., China) was employed to stain the slices for 2 min and slices were dehydrated with ethanol of 95%, 95%, 100% and 100% for 1 min. The slices were immediately soaked in carbol-xylene (RBX-8450, Shanghai Rongbai Biotechnology Co., Ltd., China) at a ratio of 3: 1 and xylene for 1 min for transparency, respectively. And then the slices were sealed with neutral resin and observed under the microscope.

### Reverse-transcription quantitative polymerase chain reaction (RT-qPCR)

Total RNA was extracted from the tissues and cells under the instruction of the RNA extraction kit (D203-01, GenStar BioSolutions Co., Ltd., China), and miR-374b, PTEN, PI3K, Akt, caspase-9, Bax, MMP2, MMP9, P53, cyclinD1, ki67, PCNA, and β-actin primers were synthesized by Takara company (Dalian, China) (Table 1). The reverse transcription system was 20 μl and the reaction conditions were set at 42℃ for 30 to 50 min (reverse transcription reaction) and at 85℃ for 5 s (reverse transcriptase inactivation reaction) with reference to the TaqMan MicroRNA Assays Reverse Transcription

Table 1. Primer sequences of related genes for RT-qPCR

| Gene | Primer sequence |
|---|---|
| miR-374b | F: 5'-ATATAATACAACCTGCTAAGTG-3' |
| | R: 5'-GTGCAGGGTCCGAGGTATTC -3' |
| U6 | F : 5'-AGAGAAGATTAGCATGGCCCCTG-3' |
| | R : 5'-ATCCAGTGCGGGTCCGAGG-3' |
| PI3K | F: 5'-AACGAGAACGTGTGCCATTTG-3' |
| | R: 5'-AGAGATTGGCATGCTGTCGAA-3' |
| Akt | F: 5'-TGAGCGACGTGGCTATTG-3' |
| | R: 5'-CAGTCTGGATGGCGGTT-3' |
| PTEN | F: 5'-TGGTGAGGTTTGATCCGCATA-3' |
| | R: 5'-CCCAGTCAGAGGCGCTATG-3' |
| caspase9 | F: 5'-GGTCGCTAATGCTGTTTCGG-3' |
| | R: 5'-GCAAGATAAGGCAGGGTGAGG-3' |
| Bax | F: 5'-CCTTTTGCTTCAGGGTTTCAT-3' |
| | R: 5'-CTCCATGTTACTGTCCAGTTCGT-3' |
| MMP2 | F: 5′-TCAGAGACGGTTGTCACAGG-3' |
| | R: 5′-GTTAAAGGAAGCACCCACCA-3' |
| MMP9 | F: 5′-GTGCTGGGCTGCTGCTTTGCTG-3′ |
| | R: 5′-GTCGCCCTCAAAGGTTTGGAAT-3′ |
| P53 | F: 5′-ATAGGATCCACCATGGAGGAGCCGAGTC -3′ |
| | R: 5′-ATAGGATCCATGTCAGTCTGAGTCAG -3′ |
| CyclinD1 | F: 5′-CTGGCCATGAACTACCTGGA -3′ |
| | R: 5′-GTCACACTTGATCACTCTGG -3′ |
| PCNA | F: 5′- GCGTGTGCCTGTGACAGTTA -3′ |
| | R: 5′-CCTAGCGTTTTTGCTTCCCTT -3′ |
| ki67 | F: 5'- GAGGGCAAGTACGAGTGGCA- 3' |
| | R: 5'- GCAGGTCGCTTCCTTATTCC- 3' |
| β-actin | F: 5' - CACCCGCGAGTACAACCTTC - 3' |
| | R: 5' - CCCATACCCACCATCACACC - 3' |

Note: RT-qPCR, reverse-transcription quantitative polymerase chain reaction miR-374b, microRNA-374b; PI3K, phosphatidylinositol 3-kinase; PTEN, phosphatase and tensin homolog deleted on chromosome 10; PCNA, proliferating cell nuclear antigen; MMP, matrix metalloproteinase; F, forward; R, reverse.

Primer (4366596, Thermo Fisher Scientific Inc., China). The reaction solution was taken for RT-qPCR, with 50 μl of reaction system including 25 μl SYBR® Premix Ex TaqTM II (2 ×) (RR820A, Xingzhi Co., Ltd., China), 2 μl PCR upstream primer, 2 μl PCR downstream primer, 1 μl ROX Reference Dye (50 ×), 4 μl DNA template and 16 μl double distilled $H_2O$. RT-qPCR was carried out using ABI PRISM® 7300 system (Applied Biosystem, USA). The reaction conditions were predenaturation at 95℃ for 10 min, 40 cycles of denaturation at 95℃ for 15 s, and annealing and extension at 60℃ for 1 min. U6 was regarded as the internal control of miR-374b, and β-actin (AA132, Beyotime Institute of Biotechnology, China) was considered as the internal control of the other genes. The $2^{-\Delta\Delta Ct}$ represented the ratio of the gene expression of the experiment group to the control group. The formula was $\Delta\Delta Ct = \Delta Ct_{\text{experiment group}} - \Delta Ct_{\text{control group}}$. When the real-time fluorescence intensity of the reaction reached the set threshold, the number of amplification cycles presented as Ct, and the amplification was at the logarithmic growth phase (This experiment was repeated for 3 times). The experiments were also applicable for cell experiments.

## Western blotting

The GIST tissues and adjacent normal tissues were added with liquid nitrogen and ground to uniform fine powder. An amount of 1 ml tissue lysate (50 mmol/l Tris, 150 mmol/l NaCl, 5 mmol/l ethylenediaminetetraacetic acid (EDTA), 0.1% sodium dodecyl sulphate (SDS), 1% NP-40, 5 μg/ml Aprotinin and 2 mmol/l PMSF) was added and ground in an ice bath, with addition of the protein lysate at 4℃ for 30 min, shaking once every 10 min. After centrifugation at 4℃ at 25764 g for 20 min, the lipid layer was discarded, and the supernatant was taken to determine the protein concentration of each sample using bicinchoninic acid (BCA) kit (20201ES76, Yeasen Biotechnology Co., Ltd., China), and deionized water was utilized to adjust the sample volume (30 μg) in protein lane. Then 10% SDS separation gel and spacer gel were prepared, the sample was mixed with the loading buffer and boiled at 100℃ for 5 min. After the ice bath and centrifugation, the samples were added into every lane with the same amount for electrophoretic separation. The protein on the gel was then transferred to the polyvinylidene difluoride (PVDF) membrane. Skim milk powder (5%) was used for blocking at 4℃ for 2 h. The membrane was placed overnight at 4℃ respectively in 1:100 mouse anti-human PTEN polyclonal antibody, rabbit anti-human Akt polyclonal antibody, mouse anti-human PI3K (P85) monoclonal antibody, rabbit anti-human caspase-9 (YK024, Shanghai Westang Biotechnology Co., Ltd., China), Bax antibody (TA337090, Zhongshan Goldenbridge Biotechnology Co., Ltd., China), cyclinD1 (ab134175, Abcam, USA), MMP2 (ab37150, Abcam, USA), MMP9 (ab76003, Abcam, USA), P53 (ab32049, Abcam, USA), ki67 (ab15580, Abcam, USA), PCNA (ab18197, Abcam, USA), and human β-actin antibody (1: 3000, PR-0255, Zhongshan Goldenbridge Biotechnology Co., Ltd., China). β-actin was the internal control. After washing the membrane with Tris-buffered saline with Tween 20 (TBST) three times (5 min each time), horseradish peroxidase (HRP)-labeled goat anti-rabbit IgG (1: 500) was used for incubation for 2 h. Then, the membrane was rewashed with TBST three times (5 min each time). The electrogenerated chemiluminescence (ECL) was employed for developing. The expression level of each protein was semi-quantified by the ratio of the grey value of target protein to the grey value of β-actin. The experiment was conducted for three times.

## Cell culture, grouping and transfection

Human GIST-T1 cell line (UFJ10931, Shanghai Junrui Biotechnology Co., Ltd., China) and human gastric mucosal epithelial cell line GES-1 (ATCC-Y2712, Shanghai Biological Technology Co., Ltd. enzyme research, China) were cultured separately. The cells were cultured with RMPI-1640 medium (GNM-31850, Shanghai Jingke Chemical Co., Ltd., China) containing 10% FBS (fetal bovine serum) (C0230, Beyotime Institute of Biotechnology, China) at 37℃ in an incubator with 5% $CO_2$.The cells were subcultured once every 2 to 3

days, and the cells in logarithmic growth phase were selected for the following experiments.

GIST-T1 and GES-1 cells were divided into the normal (GES-1 cell line), blank (GIST-T1 cell line), negative control (NC) (GIST-T1 cell line transfected with miR-374b NC sequence), miR-374b mimics (GIST-T1 cell line transfected with miR-374b mimic), miR-374b inhibitor (GIST-T1 cell line transfected with miR-374b inhibitor), siRNA-PTEN (GIST-T1 cell line transfected with siRNA-PTEN), and miR-374b inhibitor + siRNA-PTEN (GIST-T1 cell line transfected with miR-374b inhibitor and siRNA-PTEN) groups. The GIST-T1 cells were first cultured in RMPI-1640 medium containing 10% FBS in an incubator with $CO_2$ at 37℃ until the logarithmic growth phase. The cells were detached with 0.25% trypsin and inoculated into a 6-well plate with $1 \times 10^6$ cells per well. All plasmids were transfected into GIST-T1 cells using Lipofectamine™ 2000 (11668019, Thermo Fisher Scientific Inc., USA). And 100 pmol miR-374b mimics, miR-374b inhibitors, siRNA-PTEN, miR-374b inhibitors + siRNA-PTEN and NC (final concentration, 50 nM in the cells) were diluted with 250 μl serum-free Opti-MEM (31985070, Gibco®, Thermo Fisher Scientific Inc., USA). After mixing, the mixtures were incubated at room temperature for 5 min. The serum-free Opti-MEM (250 μl) was utilized to dilute 5 μl Lipofectamine™ 2000. After mixing, it was also incubated at room temperature for 5 min. Then, those two mixtures were mixed together, followed by incubation at room temperature for 20 min and added into cell culture wells. After cultivation for 6 to 8 h at 37℃ with 5% $CO_2$, complete medium was used for cultivation. The following experiments were carried out after cultivation for 24 to 28 h.

## Dual-luciferase reporter gene assay

The fragment of the target gene PTEN sequence complementary to the corresponding miR-374b was synthetized and the fragment of PTEN containing the predicted miR-374b binding site was cloned into the *Xba* I site of the pGL3 vector. The correct luciferase reporter plasmids wild type (WT) and mutant type (MUT) were then co-transfected with miR-374b to GIST-T1 cells and human gastrointestinal cells, and the NC was transfected into GIST-T1 cells and human gastrointestinal cells. The two groups were separately cultured in 24-well plates (2 ml per well). The cells were collected after transfection for 48 h. A luciferase kit (E2610, Saihongrui Biotechnology Co., Ltd., China) and a fluorescence detector (Glomax20/20, Promega Corp., USA) were used to detect the luciferase activity.

## MTT assay

GIST-T1 cells in logarithmic growth phase were selected and inoculated into the plates with 5,000 cells in each well in triplicate. MTT solution (ST316, Beyotime Institute of Biotechnology, China) (5 mg/ml) was added into each well at different time points after 24, 48, and 72 h of culture. After incubation in a $CO_2$ incubator at 37℃ for 4 h, the culture medium was discarded after centrifugation. Then, dimethyl sulfoxide (DMSO) (100 μl, ST038, Beyotime Institute of Biotechnology, China) was added and shaken for 15 min. The optical density (OD) value of each well was determined by a microplate reader at the wavelength of 570 nm. The growth curve was plotted with the OD value as the ordinate and the time as the abscissa, and the survival rate was calculated. The experiment was repeated for three times.

## Flow cytometry

After the transfection and cultivation of cells for 24 h, the culture medium was discarded and the cells were washed with phosphate-buffered saline (PBS) once. The cells were digested with 0.25% trypsin solution and the digestive solution was discarded. When the cells were observed to shrink under the microscope, the cells were added with the serum-containing medium to stop digestion. The cells were triturated to remove from the wall for suspension. The suspension was centrifuged at 178 g for 5 min, and the supernatant was discarded. The cells were washed twice with PBS solution and fixed with pre-cooled 70% ethanol for 30 min. After the centrifugation, the cells were collected. After rinsing with PBS solution, 1% propidium iodide (PI) (WB1021, Shanghai Jingke Chemical Co., Ltd., China) containing ribonuclease (RNase) was added to stain the cells for 30 min. Then the cells were washed with PBS for two times to remove PI. The volume of PBS was adjusted to 1 ml. The samples were placed in BD-Aria flow cytometry (342975, BD, USA) for detection of cell cycle, with 3 samples in each group. The experiment was repeated for three times.

At 48 h after transfection, the cells were digested with EDTA-free trypsin and collected in a flow tube. The supernatant was discarded by centrifugation. The cells were washed three times in cold PBS and the supernatant was removed after centrifugation. Annexin-V-FITC (1001-1000, Guangzhou Whiga Technology Co., Ltd., China), PI and hydroxyethyl piperazine ethanesulfonic acid (HEPES) buffer solution (CC0072, Shanghai Jingke Chemical Co., Ltd., China) were prepared for annexin-V-FITC/PI solution at the ratio of 1: 2: 50 according to the instruction of the Annexin-V-FITC Apoptosis Detection Kit. Every 100 μl of the dye solution was resuspended to $1 \times 10^6$ cells, shaken and mixed. After incubation at room temperature for 15 min, HEPES buffer solution (1 ml) was added and the mixture was shaken. Flow cytometry was employed to determine FITC and PI fluorescence at the wavelength of 488 nm for measurement of the apoptosis.

## Wound healing assay

Cells were seeded in a 6-well plate ($5 \times 10^5$ cells per well), different siRNA was added into different groups, and three wells were set. After 6 h, the medium culture was changed into normal medium culture, and a straight line on the cell surface was drawn with a ruler. After washed with PBS for three times and cultured for 48 h, cells were photographed under an inverted microscope (× 200) and the scratch distance was measured.

## Transwell assay

Matrigel was diluted with pre-cooled serum-free Dulbecco's Modified Eagle Medium (DMEM) (1: 10). The fully mixed Matrigel (356234, corning, Corning City, USA) was added into the upper chamber and stored at room temperature for

2 h. After being washed by 200 μl serum-free DMEM, cells were resuspened by serum-free DMEM after digestion, counted and diluted to $3 \times 10^5$ cells/ml. A volume of 100 μl cell solution was added into the Transwell upper chamber and 600 μl 10% serum DMEM (serum as chemokine) into Transwell lower chamber according to Transwell small chamber instruction. After 24 h incubation, the small chamber were collected and fixed by methanol for 5 min. After washed with PBS for two times, cells were observed and photographed under the eosin staining microscope, and the number of transmembrane cells was counted.

## Statistical analysis

The data were processed by SPSS 21.0 statistical software (IBM Corp., Armonk, NY, USA). The measurement data were presented in the way of mean ± standard deviation

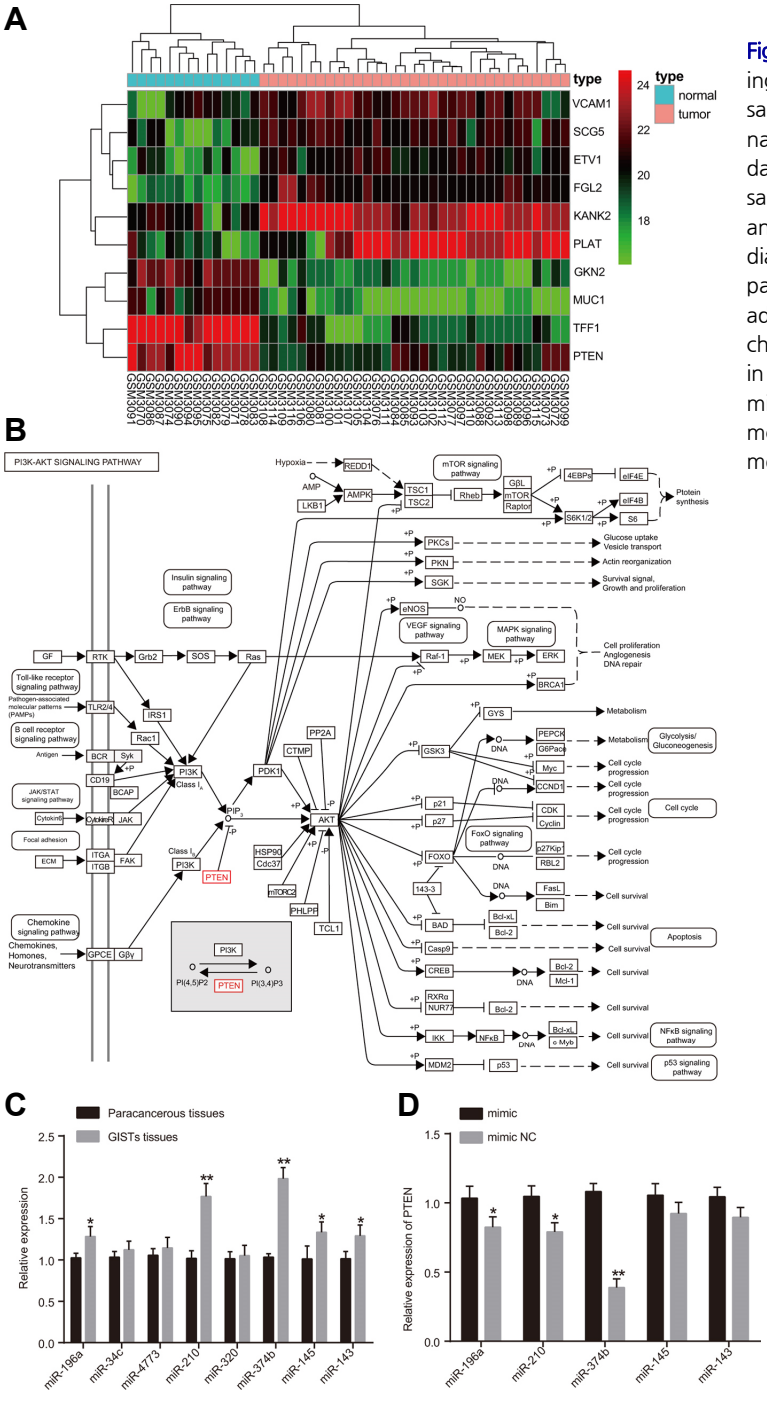


**Fig. 1. MiR-374b and PTEN were screened.** (A) Screening map of microarray data of GIST (GSE112) (the sample number as the abscissa and DEGs as the ordinate; the histogram in the upper right is the color gradation, among which each rectangle corresponds to a sample expression value, red refers to high expression, and green refers to low expression). (B) Mechanism diagram of PTEN participating in the PI3K-Akt signaling pathway. (C) Expression of miRNAs in GIST tissues and adjacent normal tissues by RT-qPCR. (D) Expression changes of PTEN after the overexpression of microRNA in the GIST-T1 cell line of GIST; $*p < 0.05$; $**p < 0.01$; miRNA, microRNA; GIST, gastrointestinal stromal tumor; RT-qPCR, reverse-transcription quantitative polymerase chain reaction.

(SD). The *t* test was used for comparisons between two groups. The ANOVA (one-way analysis of variance) was employed for comparisons among the multiple groups. A value of $p < 0.05$ was considered to be statistically significant.

## RESULTS

### MiR-374b is highly expressed and PTEN is downregulated in the GIST tissues

The expression profiling microarray data of GIST (GSE112) suggested that the expression of PTEN was significantly reduced in GIST (Fig. 1A). According to the KFGG analysis of DEGs, PTEN was involved in a variety of signaling pathways and miRs were associated with cancer development (Fig. 1B). The level of other microRNAs in the GIST tissues was detected by RT-qPCR according to several documents (Choi et al., 2010; Isosaka et al., 2015). The results showed that miR-196a, miR-210, miR-374b, miR-145, and miR-143 was highly expressed in the GIST tissues (all $p < 0.05$), and the level of miR-374b was the highest ($p < 0.01$) (Fig. 1C). Then, RT-qPCR was re-conducted to detect the level of PTEN in the GIST tissues after the upregulation of miR-196a, miR-210,

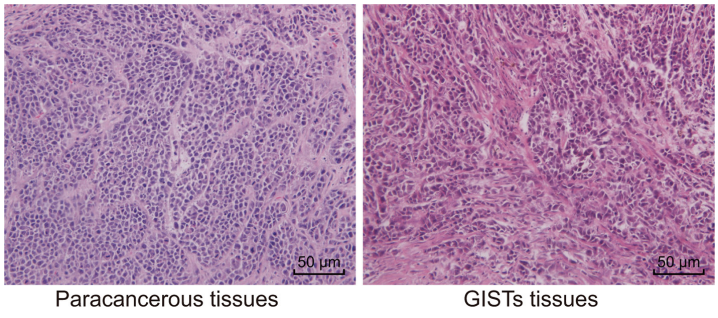


**Fig. 2. Histological changes of GIST tissues after HE staining were observed.** Note: HE, hematoxylin-eosin; GIST, gastrointestinal stromal tumor.

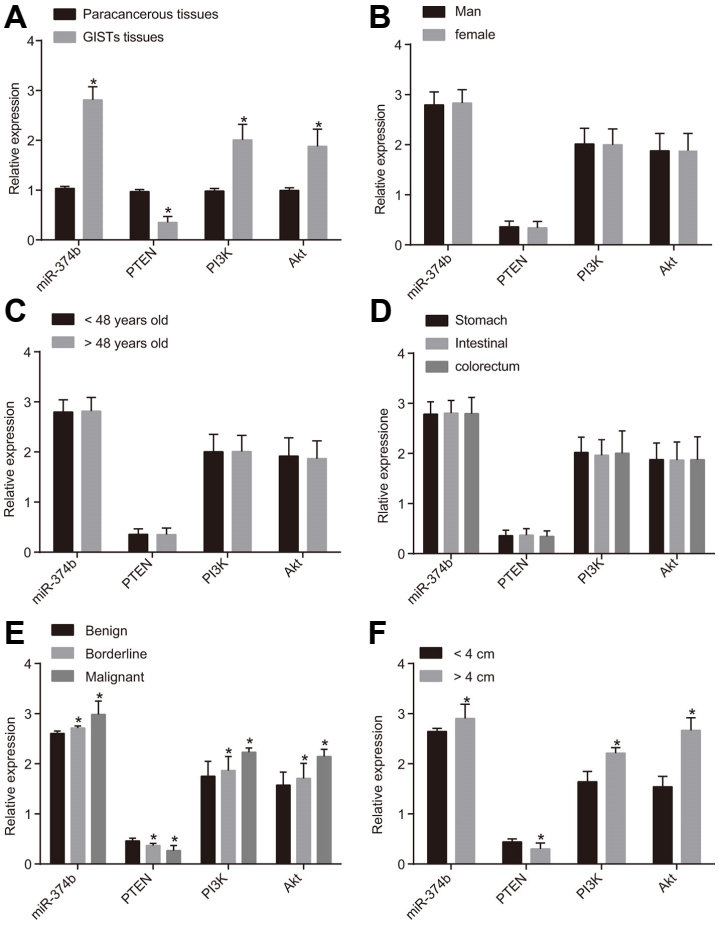


**Fig. 3. High miR-374b level and mRNA levels of PI3K and Akt, and low mRNA level of PTEN in GIST tissues by RT-qPCR.** (A) Results of miR-374b, PTEN, PI3K and Akt expressions in GIST tissues and adjacent normal tissues (*, $p < 0.05$ compared with adjacent normal tissues). (B) Results of miR-374b level and of PTEN, PI3K and Akt mRNA levels in GIST tissues with different gender. (C) Results of miR-374b level and of PTEN, PI3K and Akt mRNA levels in GIST tissues with different age. (D) Results of miR-374b level and of PTEN, PI3K and Akt mRNA levels in GIST tissues with different primary site. (E) Results of miR-374b level and of PTEN, PI3K and Akt mRNA levels in GIST tissues with different pathological stage (*$p < 0.05$, compared with benign tissues). (F) Results of miR-374b level and of PTEN, PI3K and Akt mRNA levels in GIST tissues with different tumor diameter (*$p < 0.05$, compared with tissues that tumor diameter ≤ 4 cm); miRNA, microRNA; GIST, gastrointestinal stromal tumor; RT-qPCR, reverse-transcription quantitative polymerase chain reaction; PI3K, phosphatidylinositol 3-kinase; PTEN, phosphatase and tensin homolog deleted on chromosome 10; mean ± standard deviation; the one-way ANOVA was used to analyze data; n = 3.

miR-374b, miR-145, and miR-143. All these data that the over expression of miR-196a, miR-210, and miR-374b inhibits the expression of PTEN (all $p < 0.05$), among which the overexpression of miR-374b is particularly significant ($p < 0.01$) (Fig. 1D). Thus, miR-374 was used for the follow experiments.

## Histological changes of GIST tissues are observed

Results of HE staining was shown in Fig. 2. In adjacent normal tissues, the stratification of gastrointestinal tissue was obvious, and all layers were intact without rupture or dissolution. The glands of stomach and intestines were obvious without pathological changes. The muscles were closely arranged in order. In GIST tissues, cells were in palisade, cross spiral and leaf shaped arrangement. And it presented with pink cytoplasm, specific small nuclear, rod-shaped nuclear and rounded ends. There were vacuoles in the nucleus, and some nuclei had eosinophilic nucleoli with large size, and it showed oval or multiple types accompanied by nuclear division. In addition, tumor cells can invade the mucosa or muscularis.

## Levels of miR-374b, PTEN, PI3K, and Akt correlates with the tumor diameter and pathological stage of GIST

RT-qPCR and western blotting were conducted to detect the levels of miR-374b, PTEN, PI3K, and Akt (Figs. 3 and 4). Compared to adjacent normal tissues, the miR-374b level and mRNA and protein levels of PI3K and Akt in GIST tissues were significantly increased, while PTEN mRNA and protein levels were significantly decreased (all $p < 0.05$). Compared with tissues that tumor diameter ≤ 4 cm and benign GIST tissues, the levels of miR-374b, PI3K and Akt were significantly increased in tissues that tumor diameter > 4 cm and malignant GIST tissues, while PTEN level was significantly decreased ($p < 0.05$). The levels of miR-374b, PI3K and Akt in GIST tissues were uncorrelated with age, gender and the primary site (all $p > 0.05$). All these indicated that the miR-374b level and mRNA and protein levels of PI3K, and Akt elevated in GIST tissues, and PTEN mRNA and protein levels decreased. The levels of miR-374b, PTEN, PI3K, and Akt were related to the tumor diameter and pathological stage of GIST.

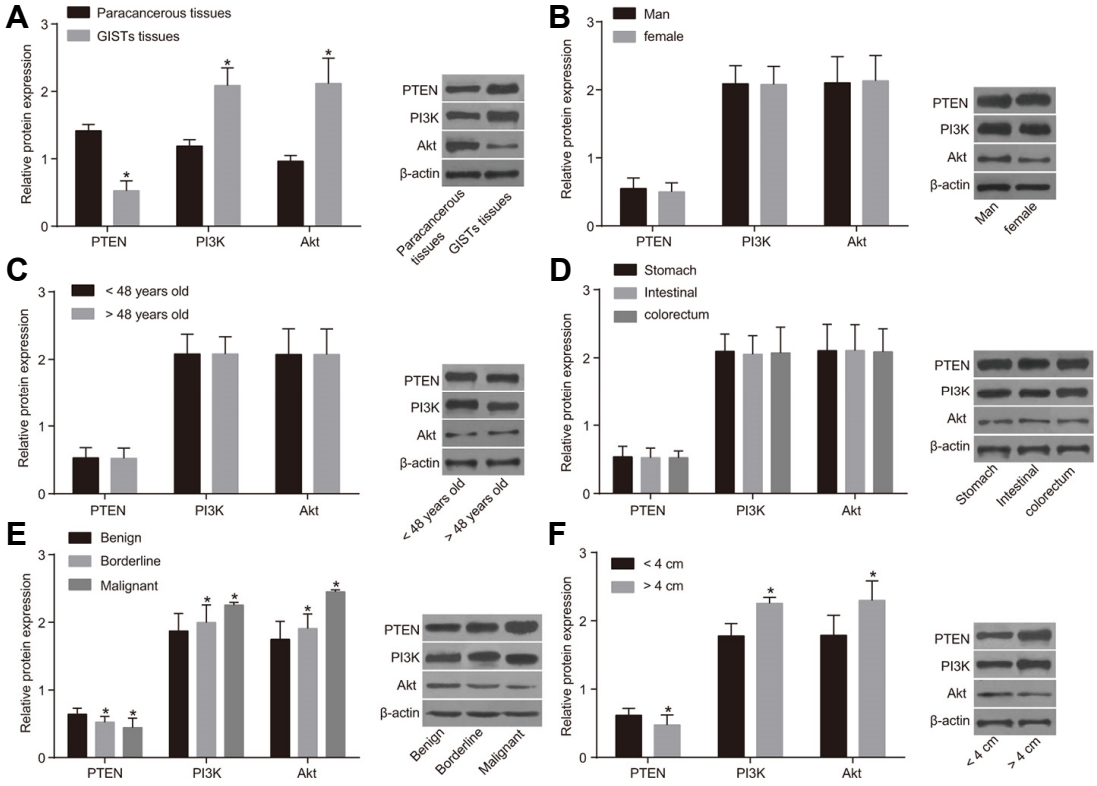


**Fig. 4. High protein levels of PI3K and Akt, and low protein level of PTEN in GIST tissues by Western blotting.** (A) Protein band graphs and results of PTEN, PI3K and Akt protein levels in GIST tissues and adjacent normal tissues (*$p < 0.05$, compared with adjacent normal tissues). (B) Protein band graphs and results of PTEN, PI3K and Akt protein levels in GIST tissues with different gender. (C) Protein band graphs and results of PTEN, PI3K and Akt protein levels in GIST tissues with different age. (D) Protein band graphs and results of PTEN, PI3K and Akt protein levels in GIST tissues with different primary site. (E) Protein band graphs and results of PTEN, PI3K and Akt protein expressions in GIST tissues with different pathological stage (*$p < 0.05$, compared with benign tissues). (F) Protein band graphs and results of PTEN, PI3K and Akt protein levels in GIST tissues with different tumor diameter (*$p < 0.05$, compared with tissues that tumor diameter ≤ 4 cm); miRNA, microRNA; GIST, gastrointestinal stromal tumor; PI3K, phosphatidylinositol 3-kinase; PTEN, phosphatase and tensin homolog deleted on chromosome 10; mean ± standard deviation; the one-way ANOVA was used to analyze data; n = 3.

### PTEN is a target gene of miR-374b

By using the website http://www.microrna.org, it was concluded that PTEN was the target gene of miR-374, and the luciferase reporter vector of PTEN and miR-374b binding site sequence and mutant sequence was obtained. To verify that the predicted target site of miR-374b was located in PTEN, a PTEN-containing luciferase plasmid was constructed and combined with the miR-374b mimics, and a negative control (NC) group was set. The results revealed that the luciferase activity of the PTEN-WT plasmid in the miR-374b mimics group was significantly lower compared with that in the NC group (all $p < 0.05$), while there was no significant decrease in the luciferase activity of the PTEN-MUT plasmid between the miR-374b mimics group and NC group ($p > 0.05$) (Fig. 5). PTEN was a direct target gene for miR-374b. Thus, miR-374b could target PTEN mRNA and negatively regulate its expression.

### MiR-374b activates PI3K/Akt signaling pathway by inhibiting PTEN in GIST-T1 cells

The levels of miR-374b, PTEN, PI3K, and Akt in GIST-T1 cells after transfection for 48 h were determined by RT-qPCR and western blotting (Fig. 6). In comparison to the normal group, the levels of miR-374b, PI3K and Akt significantly upregulated, while PTEN level significantly decreased (all $p < 0.05$). Compared with the blank and NC groups, the miR-374b level in the miR-374b inhibitors + siRNA-PTEN group decreased ($P < 0.05$), and there was no obvious changes in the levels of PTEN, PI3K, and Akt (all $p > 0.05$). The miR-374b in the miR-374b mimics group was increased. The miR-374b level in the siRNA-PTEN group was unchanged, and the levels of PI3K, and Akt were all increased (all $P < 0.05$), and level of PTEN decreased (all $p < 0.05$). The levels of miR-374b, PI3K and Akt were decreased in the miR-374b inhibitors group (all $P < 0.05$), and the PTEN level increased (all $P < 0.05$). These results suggested that miR-374b can activate the PI3K/Akt signaling pathway by inhibiting PTEN.

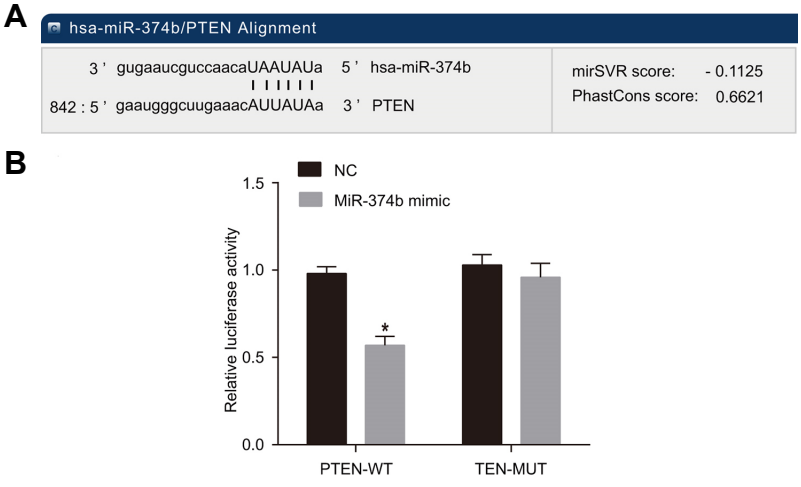


**Fig. 5. PTEN is a target gene of miR-374b.** (A) Results of biology information prediction. (B) Validation of the targeting relationship of miR-374b and PTEN genes in GIST cells; $*p < 0.05$, compared with the NC group; NC, negative control; miR-374b, microRNA-374b; GIST, gastrointestinal stromal tumor; mean ± standard deviation; the *t* test was used to analyze data; n = 3.

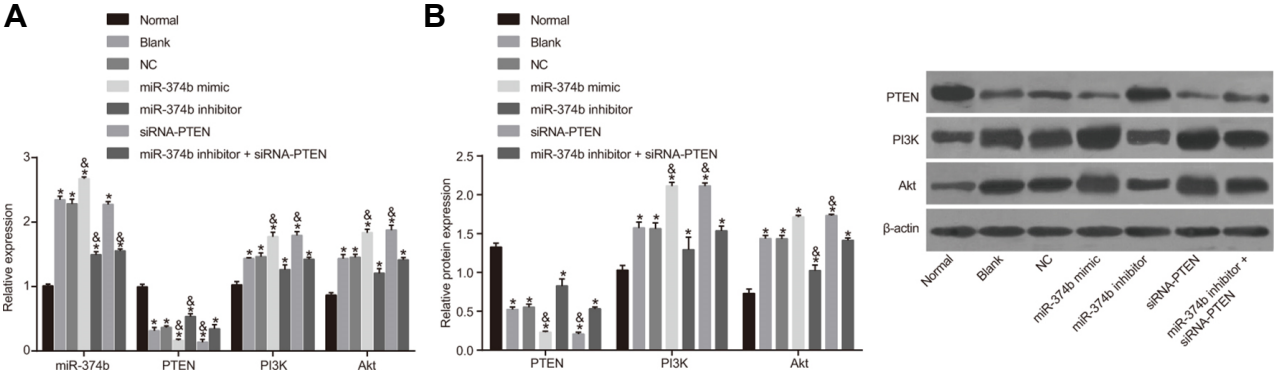


**Fig. 6. miR-374b promotes the expressions of PI3K, and Akt and inhibits the expression of PTEN.** (A) MiR-374b level and mRNA levels of PTEN, PI3K and Akt by RT-qPCR. (B) Protein levels of PTEN, PI3K and Akt by western blotting; $*p < 0.05$, compared with the normal group; $\&p < 0.05$ compared with the blank and NC groups; miR-374b, microRNA-374b; NC, negative control; RT-qPCR, reverse-transcription quantitative polymerase chain reaction; mean ± standard deviation; the *t* test was used to analyze data; n = 3.

### MiR-374b promotes viability of GIST-T1 cells by downregulating PTEN

MTT assay was conducted to measure the cell viability (Fig. 7A). Compared with the blank and NC groups, the cell viability in the miR-374b inhibitors + siRNA-PTEN group had no significant change (all $p > 0.05$); the cell viability was significantly increased in the miR-374b mimics and siRNA-PTEN groups; the cell viability in the miR-374b inhibitors group was significantly reduced (all $p < 0.05$). RT-qPCR and Western blotting were conducted to detect the expression of viability related factors, ki67 and PCNA (Figs. 7B and 7C). The levels of ki67 and PCNA had no significant difference among the blank, NC, and miR-374b inhibitors + siRNA-PTEN groups (all $p > 0.05$). Compared with the blank group, the levels of ki67 and PCNA was significantly higher in the miR-374b mimics and siRNA-PTEN groups, and the levels of ki67 and PCNA was significantly lower in the miR-374b inhibitors group. All these data suggested that miR-374b promotes viability of GIST-T1 cells through the inhibition of PTEN.

### MiR-374b inhibits apoptosis of GIST-T1 cells by downregulating PTEN

Flow cytometry was conducted to measure cell apoptosis (Fig. 8A). Compared with the blank group and NC group, the apoptosis rate in the miR-374b inhibitors group was higher, but lower in the miR-374b mimics and siRNA-PTEN groups ($p < 0.05$), and no significant changes presented in the miR-374b inhibitors + siRNA-PTEN group ($p > 0.05$). RT-qPCR and western blotting were conducted to detect the levels of Bax and caspase-9 (Figs. 8B and 8C). Compared with the blank and NC groups, the levels of Bax and caspase-9 was decreased in the miR-374b mimics and siRNA-PTEN groups (all $p < 0.05$), and the levels of Bax and caspase-9 was increased in the miR-374b inhibitors group (all $p < 0.05$). There was no significant change found in the miR-374b inhibitors + siRNA-PTEN, blank, and NC groups. The results showed that miR-374b can inhibit the apoptosis of GIST-T1 cells through the inhibition of PTEN.

### MiR-374b increases cell cycle entry of GIST-T1 cells by downregulating PTEN

Forty-eight hours after the transfection, the cell cycle each group was determined by flow cytometry (Fig. 9A). Compared with the blank and NC groups, the cells at S phase were significantly decreased and the cells at G0/G1 phase

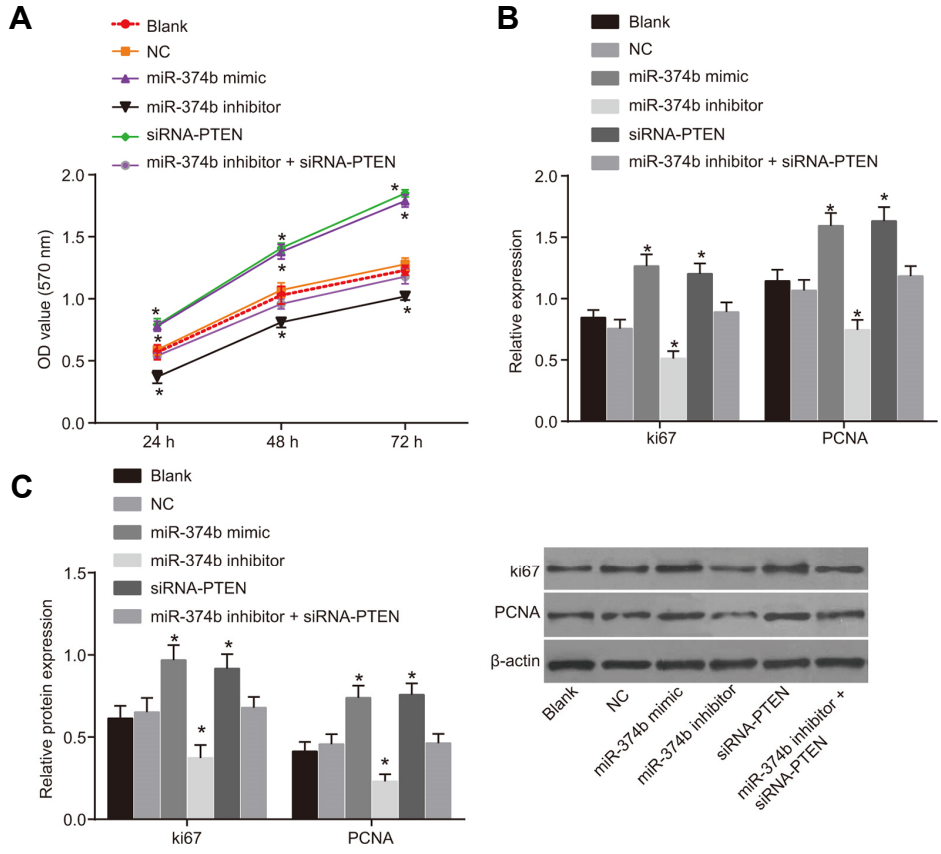


**Fig. 7. MiR-374b promotes GIST cell viability.** (A) Cell viability by MTT assay. (B) mRNA levels of ki67 and PCNA by RT-qPCR. (C) Protein levels of ki67 and PCNA by Western blotting; &$p < 0.05$, compared with the blank and NC groups; NC, negative control; miR-374b, microRNA-374b; RT-qPCR, reverse-transcription quantitative polymerase chain reaction; GIST, gastrointestinal stromal tumor; PCNA, proliferating cell nuclear antigen; mean ± standard deviation; the one-way ANOVA was used to analyze data; n = 3.

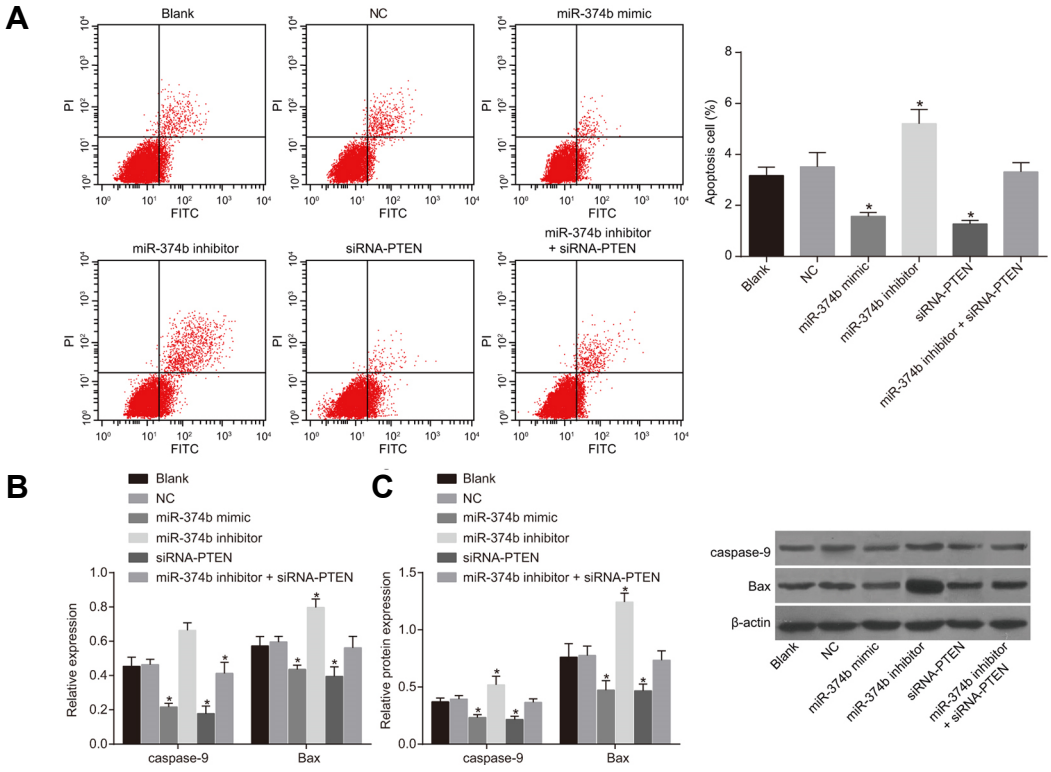


Fig. 8. MiR-374b inhibits GIST cell apoptosis. (A) Results of GIST cell apoptosis in each group by flow cytometry. (B) mRNA levels of caspase-9 and bax by RT-qPCR. (C) Protein levels of caspase-9 and bax by Western blotting; &$p < 0.05$, compared with the blank and NC groups; NC, negative control; miR-374b, microRNA-374b; RT-qPCR, reverse-transcription quantitative polymerase chain reaction; GIST, gastrointestinal stromal tumor; mean ± standard deviation; the one-way ANOVA was used to analyze data; n = 3.

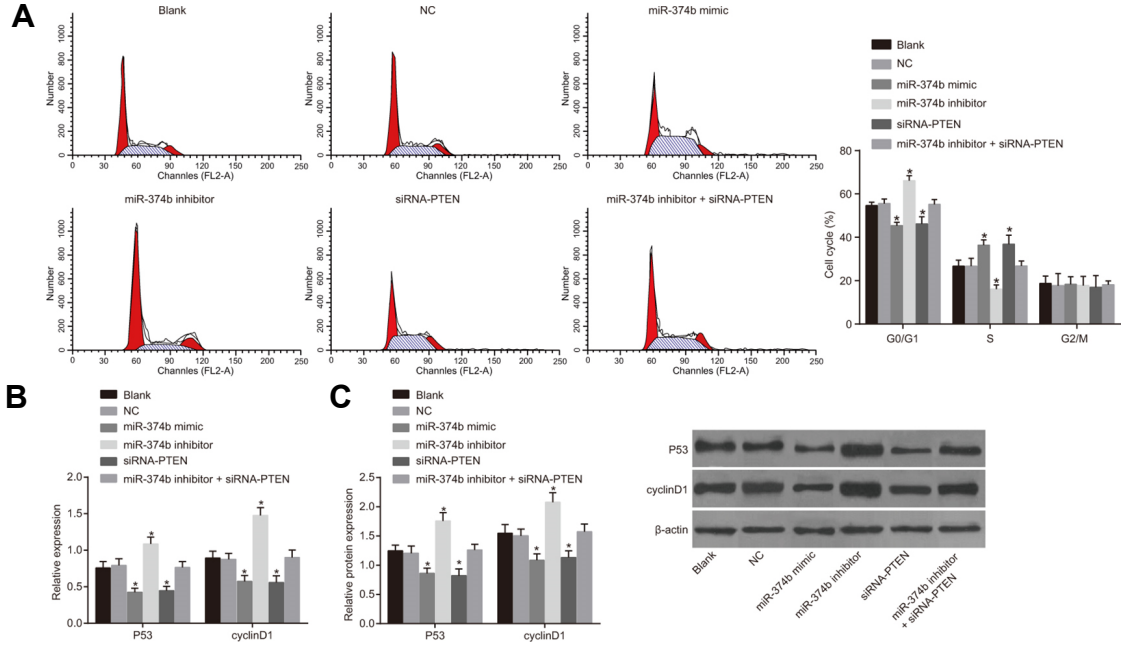


Fig. 9. MiR-374b increases GIST-T1 cell cycle entry. (A) Results of GIST cell apoptosis in each group by flow cytometry. (B) Expressions of P53 and cyclinD1 by RT-qPCR. (C) Protein levels of P53 and cyclinD1 by Western blotting; &$p < 0.05$ compared with the blank and NC groups; NC, negative control; miR-374b, microRNA-374b; RT-qPCR, reverse-transcription quantitative polymerase chain reaction; GIST, gastrointestinal stromal tumor; mean ± standard deviation; the one-way ANOVA was used to analyze data; n = 3.

were significantly upregulated in the miR-374b inhibitors group ($p < 0.05$); and the cells at S phase were significantly increased and the cells at G0/G1 phase were significantly decreased in the miR-374b mimics and siRNA-PTEN groups ($p < 0.05$). There was no significant change found in the miR-374b inhibitors + siRNA-PTEN, blank, and NC groups ($p > 0.05$). RT-qPCR and western blotting were conducted to detect the levels of P53 and cyclinD1 at 48 hour after transfection (Figs. 9B and 9C). Compared with the blank group and the NC group, the levels of P53 and cyclinD1 was increased in the miR-374b mimics and siRNA-PTEN groups (all $p < 0.05$), and the levels of P53 and cyclinD1 was decreased in the miR-374b inhibitors group (all $p < 0.05$). There was no significant change found in the miR-374b inhibitors + siRNA-PTEN, blank, and NC groups. These results indicated that MiR-374b affects GIST-T1 cell cycle entry by downregulating PTEN.

## MiR-374b promotes migration and invasion of GIST-T1 cells by downregulating PTEN

Wound healing assay was conducted to measure the cell migration ability (Fig. 10A). After transfection, the cell migration ability was increased in the blank, NC, miR-374b inhibitors, miR-374b mimics, siRNA-PTEN, and miR-374b inhibitors + siRNA-PTEN groups compared with the normal group (all $p < 0.05$). Compared with the blank and NC groups, the cell migration ability was significantly decreased in the miR-374b inhibitors group ($p < 0.05$), and was significantly increased in the miR-374b mimics and siRNA-PTEN groups ($p < 0.05$). There was no significant difference found in the miR-374b inhibitors + siRNA-PTEN, blank, and NC groups ($p > 0.05$).

Transwell assay was conducted to measure the cell invasion ability (Fig. 10B). After transfection, the cell migration ability was significantly increased in the blank, NC, miR-374b inhibitors, miR-374b mimics, siRNA-PTEN, and miR-374b inhibitors + siRNA-PTEN groups compared with the normal group ($p < 0.05$). Compared with the blank and NC groups, the cell invasion ability was significantly decreased in the miR-374b inhibitors group ($p < 0.05$), and was significantly increased in the miR-374b mimics and siRNA-PTEN groups ($p < 0.05$). There was no significant difference found in the miR-374b inhibitors + siRNA-PTEN, blank, and NC groups ($p > 0.05$).

RT-qPCR and western blotting were conducted to detect the levels of MMP2 and MMP9 (Figs. 10C and 10D). Compared with the blank NC groups, the levels of MMP2 and MMP9 was increased in the miR-374b mimics and siRNA-

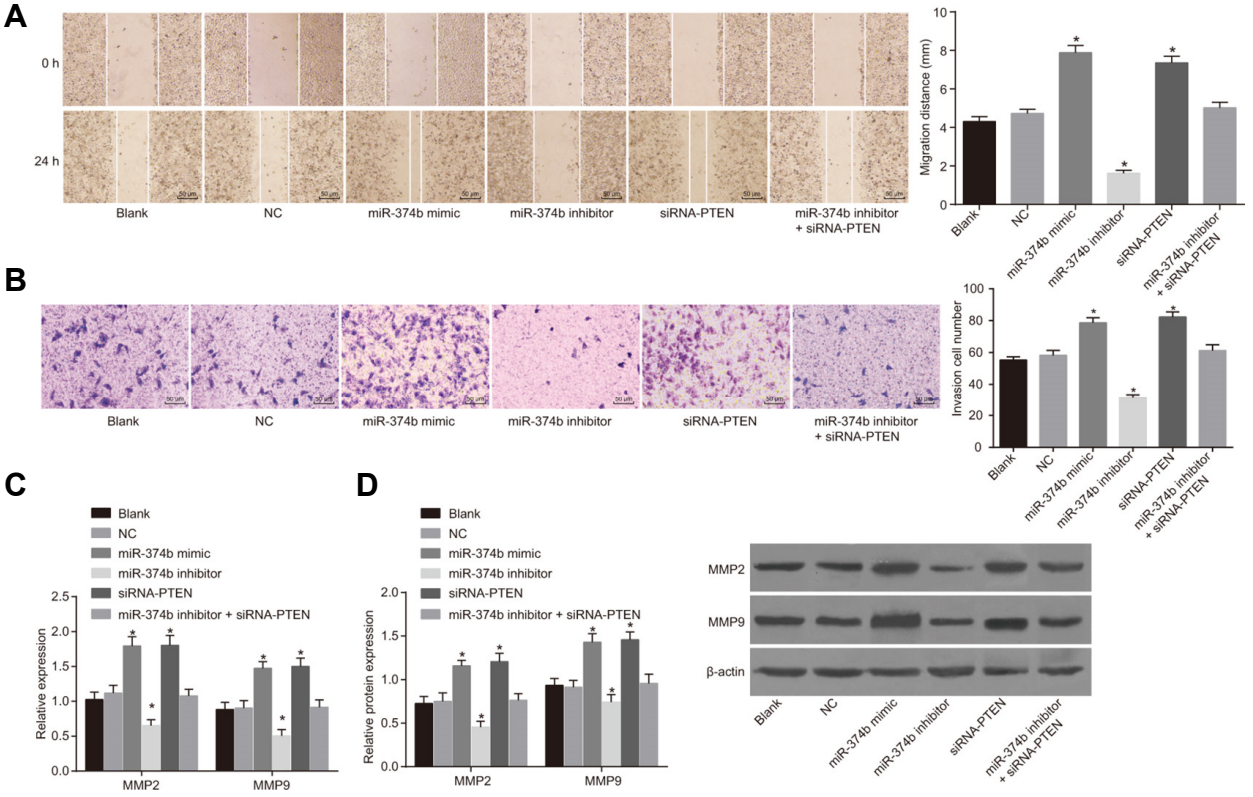


Fig. 10. MiR-374b promotes migration and invasion of GIST-T1 cells. (A) Results of cell migration in each group by wound healing assay. (B) Results of cell invasion in each group by transwell assay. (C) Expressions of MMP2 and MMP9 by RT-qPCR. (D) Protein levels of MMP2 and MMP9 by Western blotting; &$p < 0.05$, compared with the blank and NC groups; NC, negative control; miR-374b, microRNA-374b; RT-qPCR, reverse-transcription quantitative polymerase chain reaction; GIST, gastrointestinal stromal tumor; MMP, matrix metalloproteinase; mean ± standard deviation; the one-way ANOVA was used to analyze data; n = 3.

PTEN groups (all $p < 0.05$), and the levels of MMP2 and MMP9 was decreased in the miR-374b inhibitors group (all $p < 0.05$). There was no significant change found in the miR-374b inhibitors + siRNA-PTEN, blank, and NC groups ($p > 0.05$).

All these data indicated that miR-374b promotes migration and invasion of GIST-T1 cells by inhibiting PTEN.

## DISCUSSION

In order to improve the treatment for GIST and offer inspiration for new therapeutic approaches, this study was implemented to explore the effects of miR-374b and its target gene PTEN on proliferation and apoptosis of human GIST cells through the PI3K/Akt signaling pathway. In this study, we found that the expression of miR-374b and mRNA and protein expression of PI3K/Akt in tumor tissue of GIST were significantly higher in comparison to those in adjacent normal tissue, while the expression of PTEN showed the opposite trend, which indicated that inhibition of the expression of miR-374b can effectively prevent cell proliferation of GIST and promote cell apoptosis of GIST.

As the results showed, the inhibition of miR-374b expression could effectively inhibit the viability of GIST-T1 cells and promote the apoptosis of GIST-T1 cells. Genome-wide study has demonstrated that miRs can often be traced at cancer-associated genomic regions or in fragile sites, and miRs can also be found in minimal regions of loss of heterozygosity or of amplifications, or in common breakpoint regions, indicating the potential roles of miRs in tumorigenesis (Zhang et al., 2008). A previous study has reported that the diagnostic and prognostic classification of human malignancies benefit a lot from the use of miR profiles; and it has shown that many gene functions in human cancers are regulated mainly by miRs (Wu et al., 2015). Our study also proved that the expression of miR-374b in tumor tissues of GIST was significantly increased while that of PTEN was significantly decreased. A study result showed that overexpression of miR-374b resulted in the downregulation of PTEN, which accompanied with the significant increase of cell proliferation in cells (Hu et al., 2015), which is consistent with the results of our experiment. Loss of tumor suppressive miRs and/or gain of oncogenic miRs lead to tumorigenesis and progression; also, metastatic malignancy and worse prognosis of patients are more frequently associated with loss of PTEN expression. In the last decade, miRs have emerged as important regulators of a wide range of genes and signals involved in modulating epithelial-mesenchymal transition (EMT)/cancer stem cell (CSC) properties, such as the PI3K/AKT pathway (Dong et al., 2014).

With the comprehensive research of molecular biology of cancer, it has found that there are closely association among PTEN, PI3K/Akt signaling pathway and growth, proliferation, infiltration, expansion, and metastasis of malignant cells (Yang et al., 2015; Ye et al., 2017). In our study, the protein expression of PTEN in GIST tissues was significantly decreased compared with those in adjacent normal tissue, and in contrary, the protein expression of PI3K and Akt in GIST tissue was significantly increased in comparison to those in adjacent normal tissues. Interestingly, a previous study indicated that PTEN in esophageal cancer tissues presented a significantly lower expression than those in adjacent normal tissues, and PI3K/Akt in esophageal cancer tissues presented a significantly higher expression than those in adjacent normal tissues (Wu et al., 2016). PTEN is a tumor-suppressor gene that occupies a crucial position, which regulates cell growth, viability, apoptosis, mobility and signal transduction, while its expression and activity can be regulated at almost all levels: transcriptional, translational and post-translational. The function of PTEN is generally lost in a large proportion of human cancers via somatic mutations, gene silencing or epigenetic mechanisms (Xiong et al., 2016). The latest research revealed that in the PTEN/PI3K/Akt signal pathway, the activation of PI3K can catalyze 3, 4, 5-phosphatidylinositol trisphosphate phosphorylate to activate protein kinase Akt acting in the promotion of proliferation and growth of cells (Ying et al., 2015). When lacking PTEN expression, it may lead to continuous activation of signal pathway and losing control of cell growth (Li et al., 2013).

Collectively, our study proved that the inhibition of miR-374b can inhibit cell proliferation and promote cell apoptosis of GIST, which may provide a novel therapeutic target to the treatment of GIST. The correlation of miR-374b, PTEN, and PI3K/Akt signaling pathway may become new molecular markers and potential therapeutic targets which will provide certain theoretical basis for related research. In the end, due to shortage of sufficiency research data, it is essential for conducting further investigation with larger sample size and follow-up researches to validate the relationships among miR-374b, PTEN, PI3K/Akt signaling pathway, and GIST.

## ACKNOWLEDGMENTS

We would like to acknowledge the helpful comments on this paper received from our reviewers.

## REFERENCES

Cao, C.L., Niu, H.J., Kang, S.P., Cong, C.L., and Kang, S.R. (2016). miRNA-21 sensitizes gastrointestinal stromal tumors (GISTs) cells to Imatinib via targeting B-cell lymphoma 2 (Bcl-2). Eur. Rev. Med. Pharmacol. Sci. *20*, 3574-3581.

Chen, L., Wang, J., Wang, B., Yang, J., Gong, Z., Zhao, X., Zhang, C., and Du, K. (2016). MiR-126 inhibits vascular endothelial cell apoptosis through targeting PI3K/Akt signaling. Ann. Hematol. *95*, 365-374.

Choi, H.J., Lee, H., Kim, H., Kwon, J.E., Kang, H.J., You, K.T., Rhee, H., Noh, S.H., Paik, Y.K., Hyung, W. J., Kim, H. (2010). MicroRNA expression profile of gastrointestinal stromal tumors is distinguished by 14q loss and anatomic site. Int. J. Cancer *126*, 1640-1650.

Dong, P., Konno, Y., Watari, H., Hosaka, M., Noguchi, M., and Sakuragi, N. (2014). The impact of microRNA-mediated PI3K/AKT signaling on epithelial-mesenchymal transition and cancer stemness in endometrial cancer. J. Transl. Med. *12*, 231.

Fresno Vara, J.A., Casado, E., de Castro, J., Cejas, P., Belda-Iniesta, C., and Gonzalez-Baron, M. (2004). PI3K/Akt signalling pathway and cancer. Cancer Treat. Rev. *30*, 193-204.

Fujita, A., Sato, J.R., Rodrigues Lde, O., Ferreira, C.E., and Sogayar, M. C. (2006). Evaluating different methods of microarray data normalization. BMC bioinformatics *7*, 469.

Gao, Q., Ye, F., Xia, X., Xing, H., Lu, Y., Zhou, J., and Ma, D. (2009). Correlation between PTEN expression and PI3K/Akt signal pathway in endometrial carcinoma. J. Huazhong Univ. Sci. Technolog. Med. Sci. *29*, 59-63.

Hu, S., Bao, H., Xu, X., Zhou, X., Qin, W., Zeng, C., and Liu, Z. (2015). Increased miR-374b promotes cell proliferation and the production of aberrant glycosylated IgA1 in B cells of IgA nephropathy. FEBS Lett. *589*, 4019-4025.

Isosaka, M., Niinuma, T., Nojima, M., Kai, M., Yamamoto, E., Maruyama, R., Nobuoka, T., Nishida, T., Kanda, T., Taguchi, T., et al. (2015). A screen for epigenetically silenced microRNA genes in gastrointestinal stromal tumors. PloS one *10*, e0133754.

Kanehisa, M., and Goto, S. (2000). KEGG: kyoto encyclopedia of genes and genomes. Nucleic Acids Res. *28*, 27-30.

Lanke, G., and Lee, J.H. (2017). How best to manage gastrointestinal stromal tumor. World J. Clin. Oncol. *8*, 135-144.

Li, P., Mao, W.M., Zheng, Z.G., Dong, Z.M., and Ling, Z.Q. (2013). Down-regulation of PTEN expression modulated by dysregulated miR-21 contributes to the progression of esophageal cancer. Dig. Dis. Sci. *58*, 3483-3493.

Liu, G.L., Yang, H.J., Liu, B., and Liu, T. (2017). Effects of microRNA-19b on the proliferation, apoptosis, and migration of Wilms' Tumor cells via the PTEN/PI3K/AKT signaling pathway. J. Cell. Biochem. *118*, 3424-3434.

Lu, X.X., Cao, L.Y., Chen, X., Xiao, J., Zou, Y., and Chen, Q. (2016). PTEN inhibits cell proliferation, promotes cell apoptosis, and induces cell cycle arrest via downregulating the PI3K/AKT/hTERT pathway in lung adenocarcinoma A549 cells. BioMed Res. Int. *2016*, 2476842.

Maehama, T. (2007). PTEN: its deregulation and tumorigenesis. Biol. Pharmaceut. Bull. *30*, 1624-1627.

Markou, A., Zavridou, M., and Lianidou, E.S. (2016). miRNA-21 as a novel therapeutic target in lung cancer. Lung Cancer (Auckl) *7*, 19-27.

Miettinen, M., and Lasota, J. (2001). Gastrointestinal stromal tumors--definition, clinical, histological, immunohistochemical, and molecular genetic features and differential diagnosis. Virchows Archiv. *438*, 1-12.

Mogensen, C.E., and Hansen, K.W. (1990). Preventing or postponing renal disease in insulin-dependent diabetes by glycemic and nonglycemic intervention. Contrib. Nephrol. *78*, 73-100; discussion 100-101.

Sato, T., Shiba-Ishii, A., Kim, Y., Dai, T., Husni, R.E., Hong, J., Kano, J., Sakashita, S., Iijima, T., and Noguchi, M. (2017). miR-3941: A novel microRNA that controls IGBP1 expression and is associated with malignant progression of lung adenocarcinoma. Cancer Sci. *108*, 536-542.

Smyth, G.K. (2004). Linear models and empirical bayes methods for assessing differential expression in microarray experiments. Stat. Appl. Genet. Mol. Biol. *3*, Article3.

Tao, K., Yang, J., Guo, Z., Hu, Y., Sheng, H., Gao, H., and Yu, H. (2014). Prognostic value of miR-221-3p, miR-342-3p and miR-491-5p expression in colon cancer. Am. J. Transl. Res. *6*, 391-401.

Tsang, V.H., Dwight, T., Benn, D.E., Meyer-Rochow, G.Y., Gill, A.J., Sywak, M., Sidhu, S., Veivers, D., Sue, C.M., et al. (2014). Overexpression of miR-210 is associated with SDH-related pheochromocytomas, paragangliomas, and gastrointestinal stromal tumours. Endoc. Relat. Cancer *21*, 415-426.

Tu, K., Liu, Z., Yao, B., Han S., and Yang W. (2016). MicroRNA-519a promotes tumor growth by targeting PTEN/PI3K/AKT signaling in hepatocellular carcinoma. Int. J. Oncol. *48*, 965-974.

Valsangkar, N., Sehdev, A., Misra, S., Zimmers, T.A., O'Neil, B.H., and Koniaris, L.G. (2015). Current management of gastrointestinal stromal tumors: Surgery, current biomarkers, mutations, and therapy. Surgery *158*, 1149-1164.

Wang, P., Zou, F., Zhang, X., Li, H., Dulak, A., Tomko, R. J., Jr., Lazo, J.S., Wang, Z., Zhang, L., and Yu, J. (2009). microRNA-21 negatively regulates Cdc25A and cell cycle progression in colon cancer cells. Cancer Res. *69*, 8157-8165.

Wu, W. K., Lee C. W., Cho, C.H., Fan, D., Wu, K., Yu, J., and Sung, J.J. (2010). MicroRNA dysregulation in gastric cancer: a new player enters the game. Oncogene *29*, 5761-5771.

Wu, X., Li, S., Xu, X., Wu, S., Chen, R., Jiang, Q., Li, Y., and Xu, Y. (2015). The potential value of miR-1 and miR-374b as biomarkers for colorectal cancer. Int J. Clin. Exp. Pathol. *8*, 2840-2851.

Wu, Y.R., Qi, H.J., Deng, D.F., Luo, Y.Y., and Yang, S.L. (2016). MicroRNA-21 promotes cell proliferation, migration, and resistance to apoptosis through PTEN/PI3K/AKT signaling pathway in esophageal cancer. Tumour Biol. *37*, 12061-12070.

Xiong, J., Li, Z., Zhang, Y., Li, D., Zhang, G., Luo, X., Jie, Z., Liu, Y., Cao, Y., Le, Z., et al. (2016). PRL-3 promotes the peritoneal metastasis of gastric cancer through the PI3K/Akt signaling pathway by regulating PTEN. Oncol. Rep. *36*, 1819-1828.

Yang, Z., Fang, S., Di, Y., Ying, W., Tan, Y., and Gu, W. (2015). Modulation of NF-kappaB/miR-21/PTEN pathway sensitizes non-small cell lung cancer to cisplatin. PloS one *10*, e0121547.

Ye, M., Li, J., and Gong, J. (2017). PCDH10 gene inhibits cell proliferation and induces cell apoptosis by inhibiting the PI3K/Akt signaling pathway in hepatocellular carcinoma cells. Oncology Rep. *37*, 3167-3174.

Ying, J., Xu, Q., Liu, B., Zhang, G., Chen, L., and Pan, H. (2015). The expression of the PI3K/AKT/mTOR pathway in gastric cancer and its role in gastric cancer prognosis. Onco Targets Ther. *8*, 2427-2433.

Yu, G., Wang, L.G., Han, Y., and He, Q.Y. (2012). clusterProfiler: an R package for comparing biological themes among gene clusters. Omics *16*, 284-287.

Zhang, Z., Li, Z., Ga,o C., Chen, P., Chen, J., Liu, W., Xiao, S., and Lu, H. (2008). miR-21 plays a pivotal role in gastric cancer pathogenesis and progression. Lab. Invest. *88*, 1358-1366.

Zhu, C.Z., Liu, D., Kang, W.M., Yu, J.C., Ma Z.Q., Ye, X., and Li, K. (2017). Ghrelin and gastrointestinal stromal tumors. World J. Gastroenterol. *23*, 1758-1763.